Supporting Information

Mei et al. 10.1073/pnas.1717735115

SI Materials and Methods

Animals. Mice were born and reared under a 12 h light/dark condition (light intensity ~100 lx at the bottom of the cage) with food/water ad libitum and housed in groups of five. After surgery, mice were housed individually. PER2::LUC mice (1) were purchased from The Jackson Laboratory. *Cry1*$^{-/-}$ and *Cry2*$^{-/-}$ mice (2) were kindly provided by Ying Xu, Soochow University, Suzhou, Jiangsu, China. *VIP-Cre* mice (3) were kindly provided by Z. Josh Huang, Cold Spring Harbor Laboratory, New York.

Reporter Design. pAAV-EF1a-double floxed-hChR2(H134R)-mCherry-WPRE-HGHpA and AAV-EFIα-floxed-GCaMP6m were purchased from Addgene; generated AAV constructs are being deposited to Addgene for free use in academia. The AAV-P(*Cry1*)-forward-intron336-Venus-NLS-D2 reporter was cloned by replacing the EF1a promoter and the hChR2(H134R)-mCherry sequence of the pAAV-EF1a-double floxed-hChR2(H134R)-mCherry-WPRE-HGHpA plasmid by the *Cry1* promoter (the +328- to −1,208-bp region of the *Cry1* gene, transcription start site designated as "−1") and the forward-intron336-Venus-NLS-D2 sequence (intron336 refers to a functional intronic enhancer of intron1 of *Cry1*, and D2 refers to residues 422 to 461 of mouse ornithine decarboxylase) (4, 5). AAV-P(*Per2*)-DIO-mCherry-Venus-NLS-D2 was cloned by replacing the EF1a promoter of pAAV-EF1a-double floxed-hChR2(H134R)-mCherry-WPRE-HGHpA by the *Per2* promoter (+124- to −402-bp region of the *Per2* gene; transcription start site designated as "−1"); mCherry was then inserted behind the first loxP, and hChR2(H134R)-mCherry was replaced by Venus-NLS-D2. The same strategy was used to clone both AAV-P(*Per2*)-DIO-intron2-Venus-NLS-D2 and AAV-P(*Per2*)-DIO-intron2-dLUC: The promoter in AAV-P(*Cry1*)-forward-intron336-Venus-NLS-D2 was replaced by the *Per2* promoter, and the forward-intron336-Venus-NLS-D2 sequences were replaced by intron2-Venus-NLS-D2 or intron2-dLUC (intron2 refers to intron2 of *Per2* gene; dLUC was cloned from pGL4.19). AAV-P(*Cry1*)-DIO-intron336-Venus-NLS-D2 and AAV-P(*Cry1*)-DIO-intron336-dLUC were cloned by replacing the forward-intron336-Venus-NLS-D2 sequence of AAV-P(*Cry1*)-forward-intron336-Venus-NLS-D2 by the reverse complement sequence of intron336-Venus-NLS-D2 or the reverse complement sequence of intron336-dLUC.

Recombinant Adeno-Associated Viruses. All rAAVs were packaged into AAV serotype 1/2. The titers of the viruses used in the experiments of the present study ranged from 2 to 8 × 10^{12} viral particles per mL.

Stereotactic Surgery. Surgery was performed under anesthesia. rAAV (500 nL) was slowly (50 nL·min^{-1}) injected into the brain (0.46 mm posterior and 0.25 mm lateral to the bregma, and 5.7 mm from the surface of the skull for SCN; 0.46 mm posterior and 0.25 mm lateral to the bregma, and 5.0 mm from the surface of the skull for SPZ; 1.46 mm posterior and 1.0 mm lateral to the bregma, and 1.4 mm from the surface of the skull for CA1/2 of the hippocampus) by a microsyringe pump (Nanoliter 2000 Injector; WPI). Following virus injection, an optical fiber placed in a ceramic ferrule was inserted into the brain. The ceramic ferrule and the optical fiber were fixed to the skull using dental resin, and then black nail polish was smeared on the dental resin to protect against ambient light.

In Vivo Recording. Each mouse was recorded individually in a homemade box with system temperature, air, and light control (light intensity of about 100 lx at the bottom of the cage) with food/water ad libitum. Fifteen seconds of the fluorescence signal was collected once every 10 min at a 100-Hz sample rate.

Detailed in Vivo Recording System. A homemade four-channel recording instrument was used to acquire fluorescence signals from the brains of freely moving mice. A 488-nm laser (OBIS 488LS; Coherent) was coupled to a 1 × 4 beam splitter that divided the light into four laser excitation outputs of equal power. Each laser output from the beam splitter was connected to one channel of the four-channel recording instrument, which enabled us to take recordings of four animals simultaneously. The excitation laser was reflected off of a dichroic mirror (MD498; Thorlabs) and was coupled to a multimode fiber-optical patch cord (200-μm-diameter core, N.A. = 0.39, RJPSF2; Thorlabs) with an integrated rotary joint to prevent any damage to the fiber as a result of animal movement. The excitation light was then delivered into the SCN via an optical fiber (200-μm-diameter core, N.A. = 0.39, FT200EMT; Thorlabs) that was previously implanted into the SCN of the mouse brain. To minimize photobleaching during the course of long-term recording experiments, the total laser power delivered into the brain was adjusted to be as low as possible (10 to 20 μW), and the laser was only turned on during each recording session (15 s at intervals of 10 min). The emission fluorescence signals from the mouse brain were collected via the same optical fiber and were passed back through the dichroic mirror. The emissions were filtered with a band pass filter (MF525-39; Thorlabs) and were directed onto a photomultiplier tube (R3896; Hamamatsu). After amplification (voltage gain = 600 v), signals were low pass-filtered (30 Hz) and were sampled at 100 Hz with a data acquisition card (USB6009; National Instruments).

Western Blot (Half-Life Measurement). One hundred fifty nanograms of the reporter plasmid or 150 ng of the pcDNA3.1 plasmid [control (ct) panel], together with 100 ng of constitutively expressed Cre recombinase plasmid, were cotransfected into the 393T cell in one 35-mm Petri dish. Forty hours after transfection, cycloheximide (CHX) (final concentration is 100 μg/mL) or DMSO (NO CHX panel) was added, and time series samples were collected and analyzed by Western blotting. Venus and tubulin antibodies were purchased from Abcam (ab1218 and ab7291).

SCN Slice Preparation. In the ex vivo experiment, mice were reared under LD conditions (12 h light, 12 h dark). All mice were euthanized by cervical dislocation and decapitated 4 to 6 h before the light was turned off to reduce any phase shift that could occur during slice preparation (6, 7). *VIP-Cre* mice injected with AAV-P(*Per2*)-DIO-intron1-dLUC or AAV-P(*Cry1*)-DIO-intron336-dLUC virus were killed 1 mo after the injection. Then, 200-μm brain slices were immediately prepared using a Leica VT1000S vibratome. Samples were prepared in cooled Hanks' balanced salt solution (7). Dissected bilateral SCN slices were put on culture plate inserts (Milicell-CM; Millipore Corporation) in a 35-mm Petri dish with 1.2 mL of DMEM (with 0.1 mM D-luciferin Na^+ and 5% B27 supplement) and were cultured at 36 °C.

Luminescence ex Vivo Imaging and Recording. For the SCN luminescence ex vivo imaging, images were taken by an Olympus IX70 microscope using a UPlanApo 10× objective and an Andor iKon Deep Cold camera cooled to −90 °C, with 2 × 2 binning and 30-min exposure time, and then successive pairs

of images were averaged to get one image per hour. For the SCN ex vivo recording, bioluminescence was detected from the SCN for 1 min, at 10-min intervals, with a Lumicycle luminometer (Actimetrics). The time at which the light was turned on during the SCN slice preparation was defined as the start of day 0.

Fluorescence ex Vivo Imaging. For the SCN fluorescence ex vivo imaging, images were taken with a spinning disk confocal using a Super Plan-Fluar 10× objective. Images were taken every hour with an exposure duration of 500 ms. Images of 100-μm depth in the *z* axis were obtained at 10-μm *z* steps, and then the *z* steps were combined to get one image every hour.

TUNEL Assay. For the evaluation of the potential phototoxicity, a TUNEL assay was used to test the cell apoptosis 1 wk after the fiber recording. Mice were anesthetized and perfused for 1 h with 4% paraformaldehyde in PBS immediately after the fiber recording. Brains were dehydrated with 30% sucrose in PBS overnight. Then, 30-μm-thick coronal brain sections were cut using a Leica cryostat. Following rinsing twice with PBS, coronal sections were incubated in PBS with 0.3% Triton X-100 for 3 h and then washed with PBS for 10 min three times. For the positive control, slices were incubated with DNase for 5 h. Then, the slices were incubated with the TUNEL assay solution (C1089; Beyotime) for 2 h. The slices were then mounted onto slides and stained with DAPI. Fluorescence signals were visualized using a ZEISS LSM 880 confocal.

Immunohistochemistry. For VIP staining, 2 wk after injecting the fluorescence reporter AAV into the SCN of *VIP-Cre* mice, the mice were anesthetized and perfused with 4% paraformaldehyde in PBS. For GFAP staining, animals were killed 3 mo after fiber implantations. Brains were dehydrated with 30% sucrose in PBS. Serial 30-μm-thick coronal sections of the brain were made using a Leica cryostat. Nonspecific antibody binding was blocked by 60-min incubation with BSA at room temperature. Slices were incubated using primary antibodies against VIP (1:100 dilution; EMD Millipore) or GFAP (1:500 dilution, ab7260; Abcam:) overnight and then incubated with a goat anti-rabbit secondary antibody (1:500 dilutions, ab6719). The slices were then mounted onto slides and stained with DAPI. Fluorescent images were acquired using a ZEISS LSM 880 confocal.

Histological Examination. After in vivo recording and wheel-running activity measurement, mice were anesthetized and perfused with 4% paraformaldehyde in PBS. Brains were dehydrated with 30% sucrose in PBS. Serial 50-μm-thick coronal sections of the brain were made using a Leica cryostat and were stained with DAPI and scanned with an Olympus VS120 microscope with 10× objective to identify the placement of the optical fiber tip.

1. Yoo SH, et al. (2004) PERIOD2:LUCIFERASE real-time reporting of circadian dynamics reveals persistent circadian oscillations in mouse peripheral tissues. *Proc Natl Acad Sci USA* 101:5339–5346.
2. Shi G, et al. (2013) Dual roles of FBXL3 in the mammalian circadian feedback loops are important for period determination and robustness of the clock. *Proc Natl Acad Sci USA* 110:4750–4755.
3. Taniguchi H, et al. (2011) A resource of Cre driver lines for genetic targeting of GABAergic neurons in cerebral cortex. *Neuron* 71:995–1013.
4. Li X, et al. (1998) Generation of destabilized green fluorescent protein as a transcription reporter. *J Biol Chem* 273:34970–34975.
5. Ukai-Tadenuma M, et al. (2011) Delay in feedback repression by cryptochrome 1 is required for circadian clock function. *Cell* 144:268–281.
6. Davidson AJ, Castanon-Cervantes O, Leise TL, Molyneux PC, Harrington ME (2009) Visualizing jet lag in the mouse suprachiasmatic nucleus and peripheral circadian timing system. *Eur J Neurosci* 29:171–180.
7. Savelyev SA, Larsson KC, Johansson AS, Lundkvist GB (2011) Slice preparation, organotypic tissue culturing and luciferase recording of clock gene activity in the suprachiasmatic nucleus. *J Vis Exp* 48:2439.

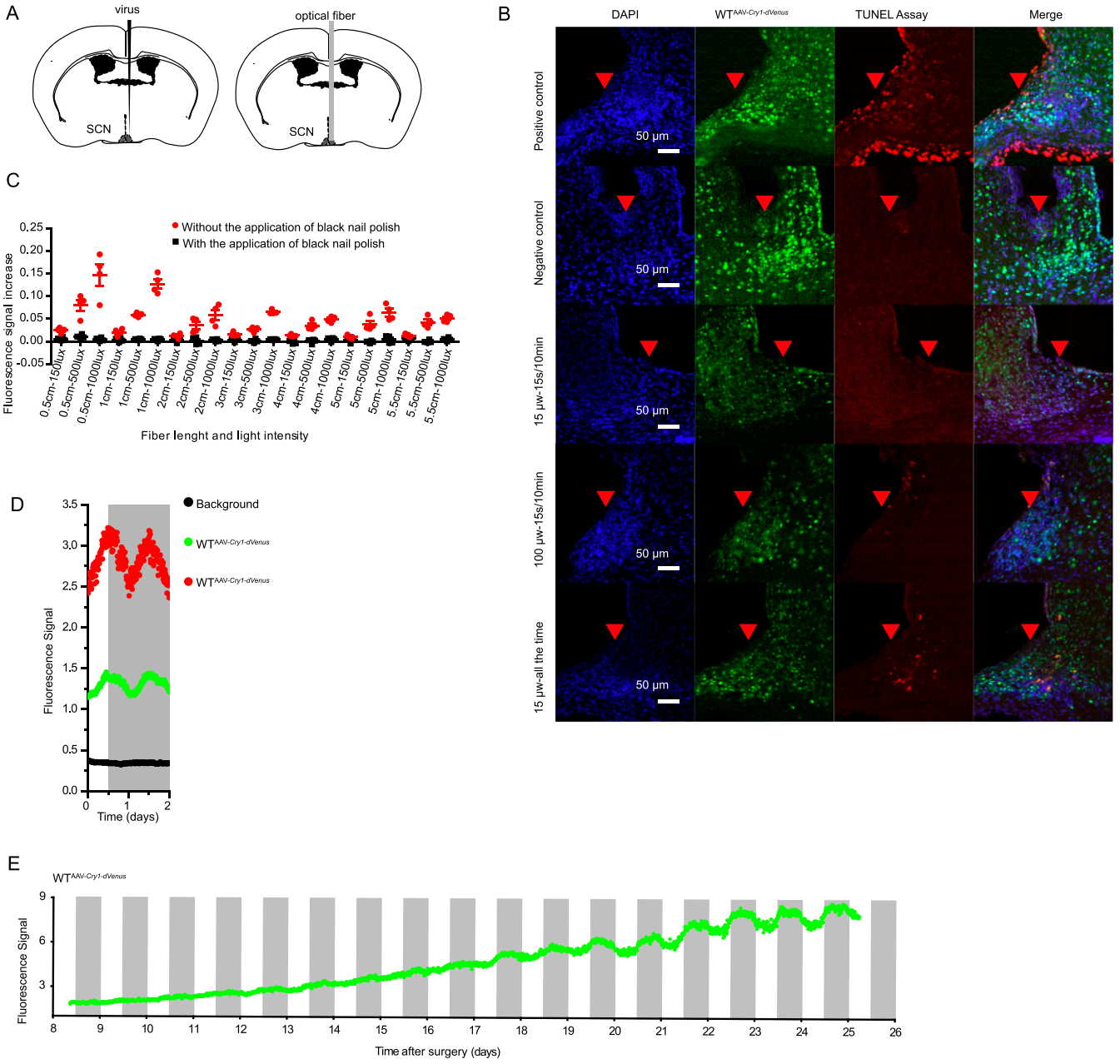

Fig. S1. Background of in vivo recording and *Cry1* transcription reporter in vivo recording in the SCN of WT mouse. (*A*) Drawings illustrate AAV virus injection (*Left*) and optical fiber insertion (*Right*). (*B*) TUNEL assay tested phototoxicity-induced cell apoptosis after 1-wk fiber recording. For positive control (*First Row*), slices were treated with DNase; for negative control (*Second Row*), laser was turned off; for the third panel, mice were recorded with 15-μW laser power turned on for 15 s every 10 min; for the *Fourth Row*, mice were recorded with 100-μW laser power turned on for 15 s every 10 min; for the *Fifth Row*, mice were recorded with 15-μW laser power turned on all of the time. The red triangles in the brain slices show the tip position of the optical fiber. (*C*) Signal noise detected by optical fiber at different depths under different levels of ambient light intensity. Every dot represents one mouse. (*D*) Background signal and two recordings of *Cry1* transcription reporter rhythm in the SCN of WT mice for 1 d in the LD condition and 1 d in the DD condition. Recording started 1 mo after the surgery; the day of the recording start was defined as day 0. The white and gray areas indicate the lights-on and lights-off periods, respectively. Raw data are plotted at 10-min intervals. (*E*) Fluorescence signal of the *Cry1* reporter in the SCN after rAAV injection. Recording started on the eighth day after surgery. The white and gray areas indicate the lights-on and lights-off periods, respectively. Raw data are plotted at 10-min intervals.

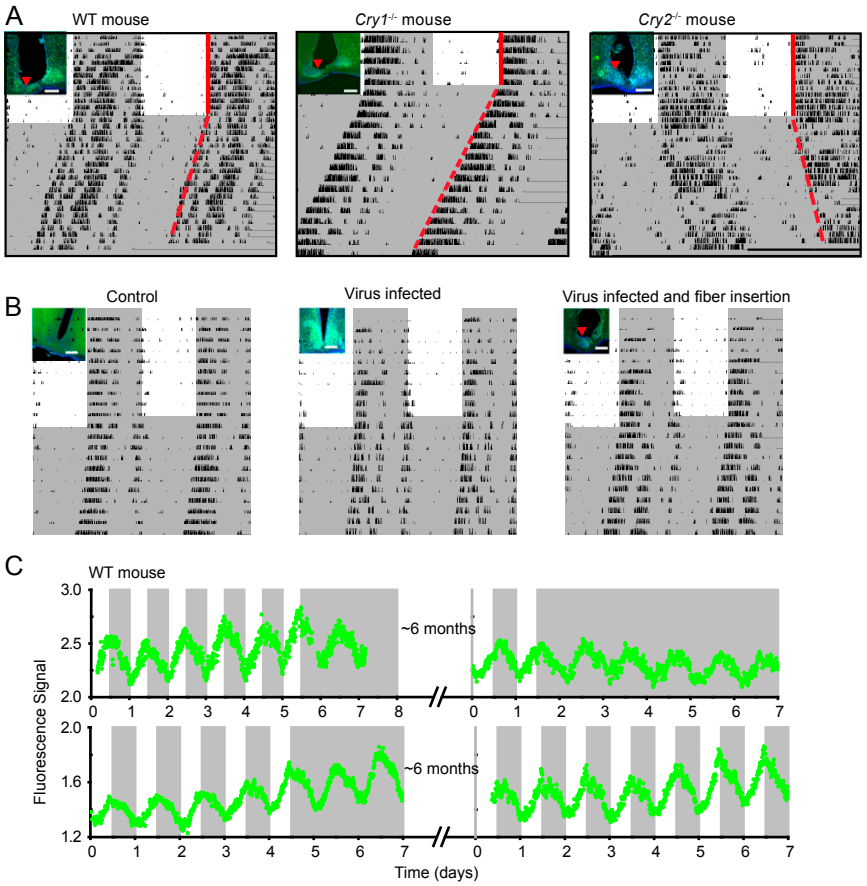

Fig. S2. Locomotor activity rhythm in WT, *Cry1*$^{-/-}$, and *Cry2*$^{-/-}$ mice and long-term in vivo recordings of *Cry1* transcription rhythms in the SCN of WT mice. (*A*) Wheel-running activity profiles of WT, *Cry1*$^{-/-}$, and *Cry2*$^{-/-}$ mice. The histological examination images are shown at the *Top Left* of each subpanel. Red triangles indicate the tip position of the optical fiber. (Scale bars: 200 μm.) (*B*) Wheel-running activity profiles of mice without surgery (*Left*), with AAV injection in the SCN (*Middle*), and with both AAV injection and fiber implantation in the SCN (*Right*). The histological examination slices are shown at the *Top Left* of each subpanel. Red triangles indicate the tip position of the optical fiber. (Scale bars: 200 μm.) (*C*) Long-term recording of *Cry1* transcription in the SCN of WT mice. The white and gray areas indicate the lights-on and lights-off periods, respectively. Raw data are plotted at 10-min intervals.

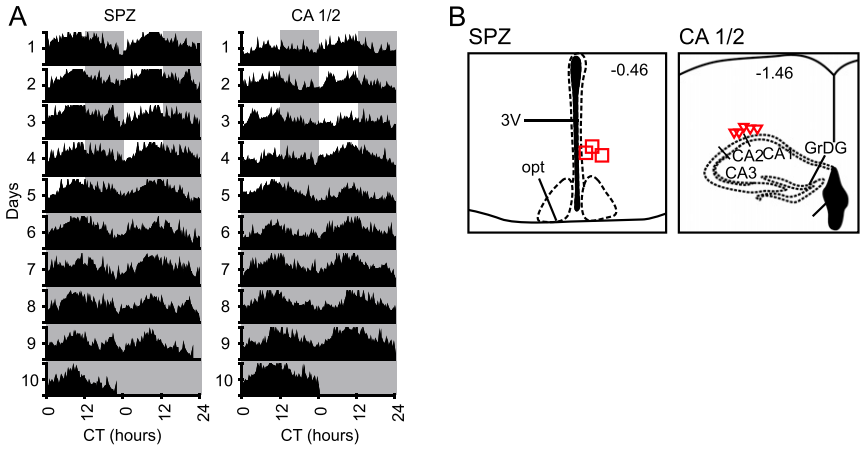

Fig. S3. Double-plotted in vivo recordings of *Cry1* transcription rhythms in the SPZ and hippocampus CA1/2 regions. (*A*) *Cry1* transcription rhythms in the SPZ and CA1/2 of WT mice presented as histograms of the mean fluorescence intensity over 15-s sampling windows (double-plotted). (*B*) The illustrations present the exact distribution of the locations of optical fiber tips for recording in the SPZ (*Left*) and CA1/2 (*Right*) of WT mice. The red triangles and red boxes in the brain slices show the tip position of the optical fiber. $n = 3$ for SPZ, and $n = 5$ for CA 1/2. GrDG, granular layer of dentate gyrus; opt, optic chiasm.

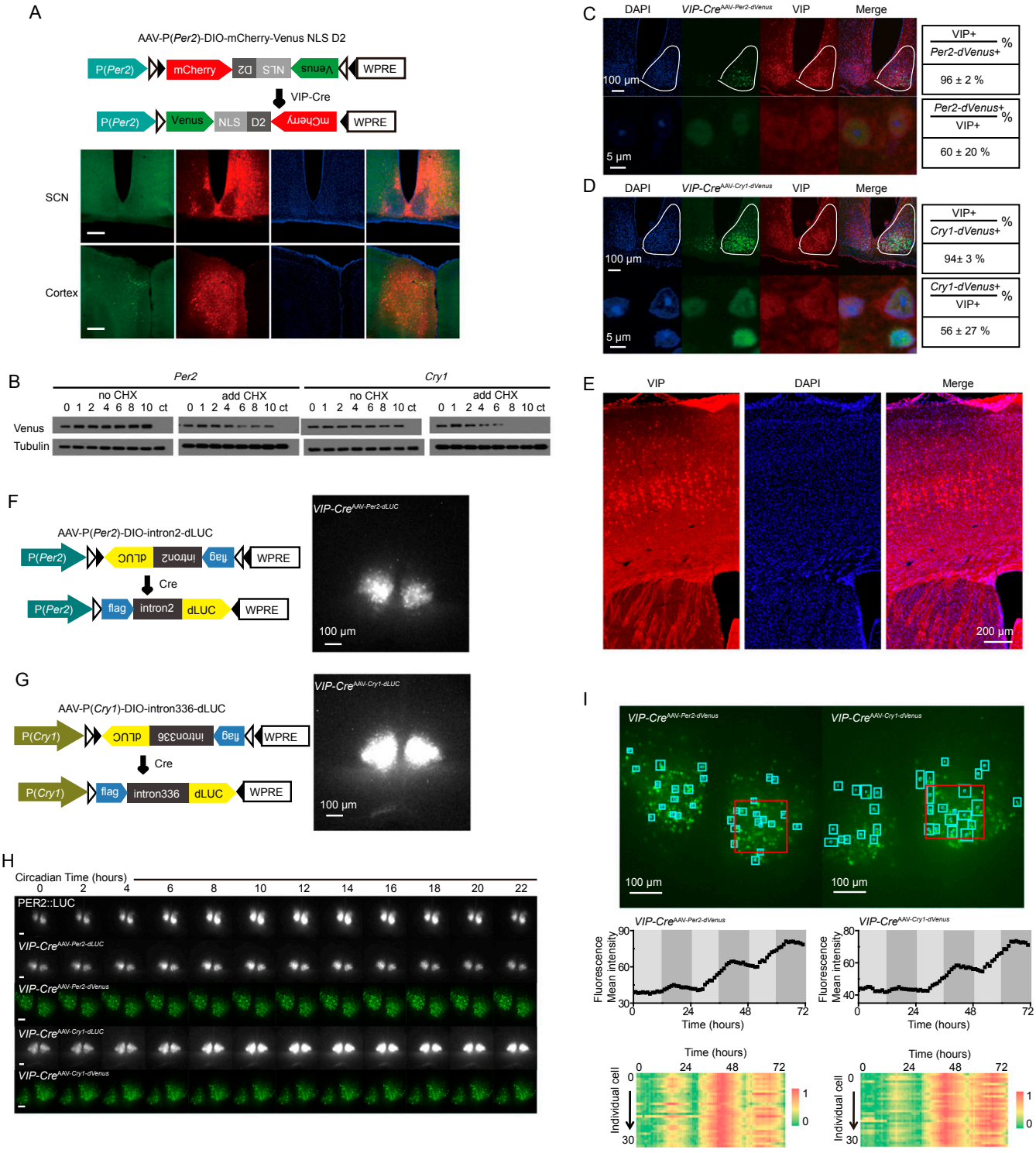

Fig. S4. In vivo and ex vivo reporter design and analysis of expression in SCN. (*A*) Expression of the *Per2* reporter that lacked intron2 in the SCN and the cortex of VIP-Cre mice. (Scale bars: 200 μm.) (*B*) Western blot result showing the half-life of the fluorescent reporters used for in vivo recordings in *VIP-Cre* mice. (*C*) Selective expression of dVenus (green) in VIP neurons (red) following unilateral injections of *AAV-Per2-dVenus* into VIP-Cre mice. *Top* was captured at a low magnification, and *Bottom* was captured at a high magnification. (Scale bars: *Top*, 100 μm; *Bottom*, 5 μm.) Quantitative data are shown at *Right*. SCN nuclei were indicated by the white lines. (*D*) Selective expression of dVenus (green) in VIP neurons (red) following unilateral injections of *AAV-Cry1-dVenus* into VIP-Cre mice. *Top* was captured at a low magnification, and *Bottom* was captured at a high magnification. (Scale bars: *Top*, 100 μm; *Bottom*, 5 μm.) Quantitative data are shown at *Right*. SCN nuclei were indicated by the white lines. (*E*) Immunolabeling of the VIP neurons (red) in the cortex. (*F*) The designs of the *Per2* ex vivo luminescent transcription reporters (*Left*) and its expression profiles in *VIP-Cre* mice (*Right*). (*G*) The designs of the *Cry1* ex vivo luminescent transcription reporters (*Left*) and its expression profiles in *VIP-Cre* mice (*Right*). (*H*) Fluorescence and luminescence SCN ex vivo image from (top to bottom) PER2::LUC, *VIP-Cre*$^{AAV\text{-}Per2\text{-}dLuc}$, *VIP-Cre*$^{AAV\text{-}Per2\text{-}dVenus}$, *VIP-Cre*$^{AAV\text{-}Cry1\text{-}dLUC}$, and *VIP-Cre*$^{AAV\text{-}Cry1\text{-}dVenus}$ mice. The circadian time is indicated at the top. Circadian time 0 is lights on. (*I*) Ex vivo fluorescent SCN slices (*Top*) indicating areas of 30 selected single cells (cyan boxes) and the overall signal (red box). Fluorescence recording in the red box of ex vivo SCN slices (*Middle*) and 30 single cell rhythm heat map results (*Bottom*), in which fluorescence intensity is color-coded as indicated, and each horizontal raster line represents recording of a single cell over time. Normalized data are plotted at 1-h intervals.

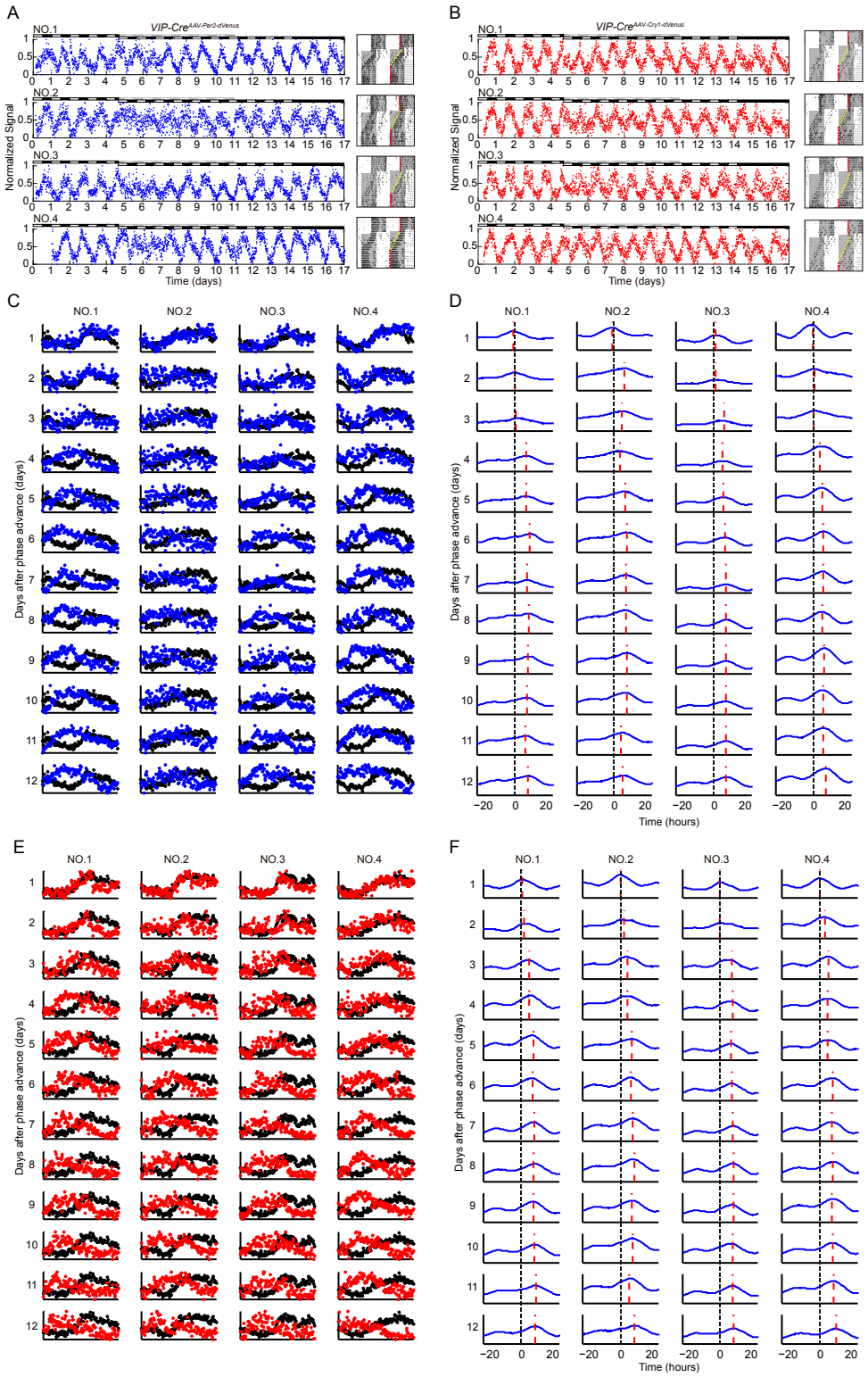

Fig. S5. In vivo monitoring of *Per2*, *Cry1* reentrainment and the cross-correlation analysis results. (*A*) Normalized *Per2* transcription profiles in SCN VIP neurons of four individual *VIP-Cre*$^{AAV\text{-}Per2\text{-}dVenus}$ mice (*Left*) and their wheel-running profiles (*Right*). (*B*) Normalized *Cry1* transcription profiles in SCN VIP neurons of four individual *VIP-Cre*$^{AAV\text{-}Per2\text{-}dVenus}$ mice (*Left*) and their wheel-running profiles (*Right*). (*C*) Alignment between the template data (black, an average of normalized data on initial days 1 to 3) and the normalized *Per2* transcription data (blue) of each day after the 8-h phase advance. (*D*) Cross-correlation results of four individual *VIP-Cre*$^{AAV\text{-}Cry1\text{-}dVenus}$ mice. The dashed black lines indicate the peak times before the 8-h phase advance, and the dashed red lines indicate the peak times of each day after the 8-h phase advance. (*E*) Alignment between the template data (black, an average of normalized data on initial days 1 to 3) and the normalized *Cry1* transcription data (red) of each day after the 8-h phase advance. (*F*) Cross-correlation results of four individual *VIP-Cre*$^{AAV\text{-}Cry1\text{-}dVenus}$ mice. The dashed black lines indicated the peak times before the 8-h phase advance, and the dashed red lines indicated the peak times of each day after the 8-h phase advance.

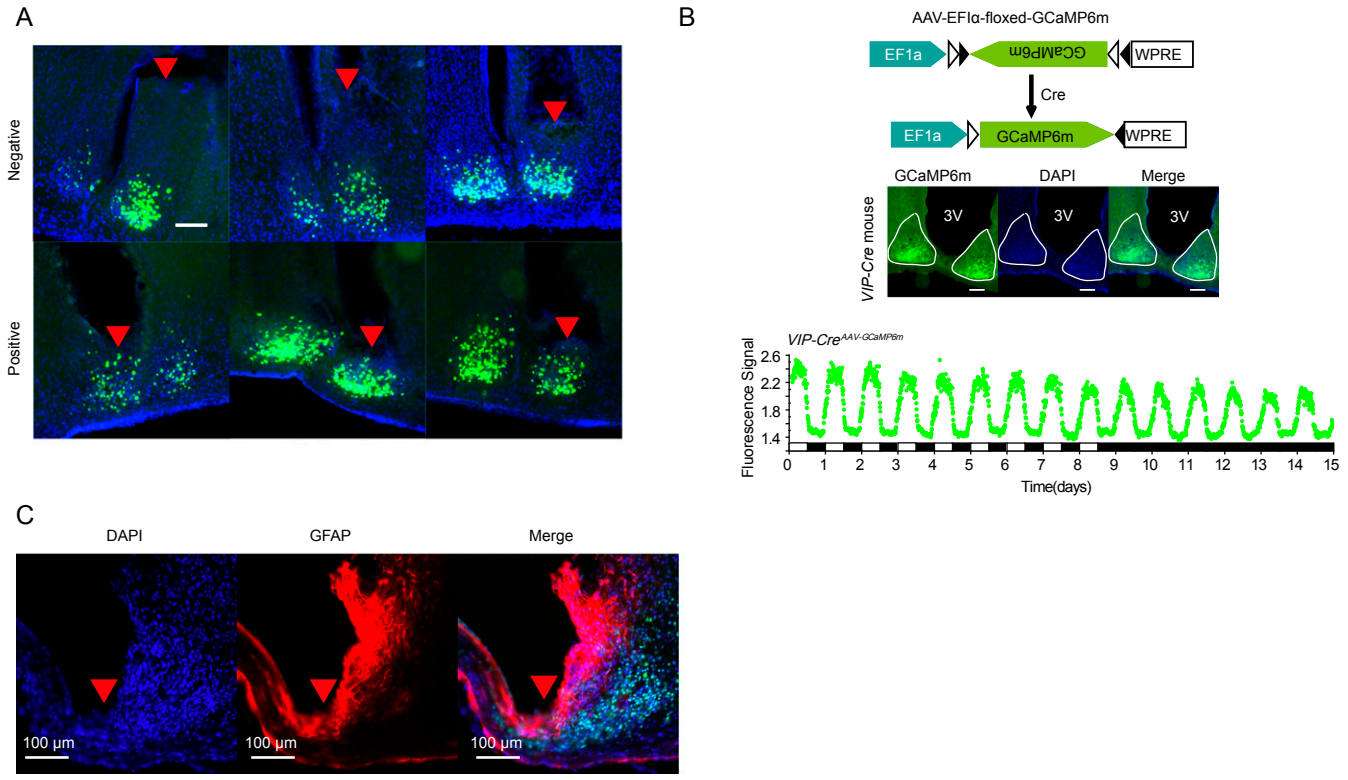

Fig. S6. In vivo recording of Ca^{2+} rhythm in SCN VIP neurons and the neuroinflammation caused by fiber implantation. (*A*) Representative images show fiber probe positions in the SCN of *VIP-Cre*$^{AAV\text{-}Per2\text{-}dVenus}$ mice that detected good (*Bottom*, n= 3 mice) or none (*Top*, *n* = 3 mice) fluorescence signals. (Scale bar: 100 μm.) (*B*) Schematic of floxed GCaMP6m virus vector (*Top*). Expression of GCaMP6m in the *VIP-Cre* mouse (*Middle*). (Scale bar, 200 μm.) Long-term in vivo recording of GCaMP6m signal in *VIP-Cre* mouse (*Bottom*). The light condition is indicated at the bottom of the figure: open bars indicate lights on, and closed bars indicate lights off. Raw data are plotted at 10-min intervals. (*C*) GFAP staining (red) in the SCN of fiber-implanted animals. Red triangles indicate the tip position of the optical fiber.

Table S1. Summary of circadian period determination in WT mouse (group data)

Sample condition	n	Mean, h	SD, h	Lower limit, h	Upper limit, h	Range, h
Control mice without surgery (locomotor activity)	4	23.90	0.07	23.83	23.99	0.16
Mice with virus injection (locomotor activity)	4	23.93	0.04	23.88	23.99	0.11
Mice with virus injection and fiber insertion (locomotor activity)	4	23.91	0.07	23.81	23.96	0.15
Mice (WT$^{AAV\text{-}Cry1\text{-}dVenus}$) SCN in vivo recording in DD condition (In vivo optical fiber recording)	4	23.92	0.06	23.85	23.98	0.13

Table S2. Summary of circadian peak phase determination in VIP-Cre mouse (group data)

Sample condition	n	Mean, h	SD, h	Lower limit, h	Upper limit, h	Range, h
Mouse in vivo LD condition						
VIP-Cre $^{AAV\text{-}Per2\text{-}dVenus}$	13	17.5	0.7	16.5	19.3	2.8
VIP-Cre $^{AAV\text{-}Cry1\text{-}dVenus}$	16	17.2	1.4	15.0	20.0	5.0
Mouse in vivo DD condition						
VIP-Cre $^{AAV\text{-}Per2\text{-}dVenus}$	7	16.1	1.2	14.7	18.1	3.5
VIP-Cre $^{AAV\text{-}Cry1\text{-}dVenus}$	8	15.8	1.7	14.0	19.0	5.0
SCN slice ex vivo						
VIP-Cre $^{AAV\text{-}Per2\text{-}dLUC}$	20	10.7	1.5	7.4	14.8	7.3
VIP-Cre $^{AAV\text{-}Cry1\text{-}dLUC}$	17	13.9	1.3	12.1	16.1	4.0
PER2::LUC	22	14.4	1.6	10.1	16.7	6.7
VIP-Cre $^{AAV\text{-}Per2\text{-}dVenus}$	3	16.3	0.3	15.7	16.7	1.0
VIP-Cre $^{AAV\text{-}Cry1\text{-}dVenus}$	3	17.2	0.3	16.7	17.7	1.0

Table S3. Summary of circadian period determination in VIP-Cre mouse (group data)

Sample condition	n	Mean, h	SEM, h	Lower limit, h	Upper limit, h	Range, h
Mouse in vivo LD condition						
VIP-Cre$^{AAV\text{-}Per2\text{-}dVenus}$	13	23.9	0.1	23.5	24.2	0.7
VIP-Cre $^{AAV\text{-}Cry1\text{-}dVenus}$	16	24.0	0.1	23.2	25.5	2.3
Mouse in vivo DD condition						
VIP-Cre $^{AAV\text{-}Per2\text{-}dVenus}$	7	23.7	0.1	23.2	24.0	0.8
VIP-Cre $^{AAV\text{-}Cry1\text{-}dVenus}$	8	23.7	0.2	22.9	24.2	1.4
SCN slice ex vivo						
VIP-Cre $^{AAV\text{-}Per2\text{-}dLUC}$	20	24.3	0.2	22.7	25.8	3.2
VIP-Cre $^{AAV\text{-}Cry1\text{-}dLUC}$	17	24.3	0.1	23.8	24.9	1.1
PER2::LUC	22	24.9	0.1	23.9	26.0	2.1
VIP-Cre $^{AAV\text{-}Per2\text{-}dVenus}$	3	24.3	0.1	24.1	24.4	0.4
VIP-Cre $^{AAV\text{-}Cry1\text{-}dVenus}$	3	24.1	0.1	24.0	24.3	0.3

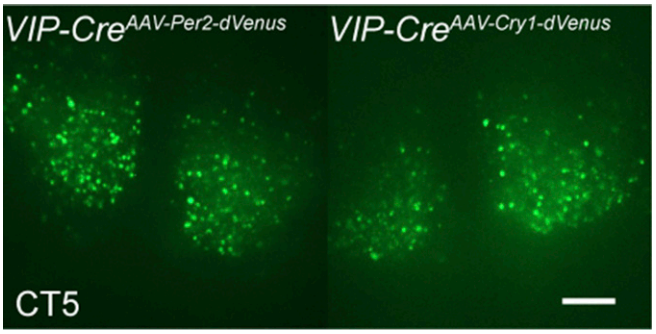

Movie S1. Representative images of circadian rhythms of VIP-CreAAV-Per2-dVenus (*Left*) and VIP-Cre AAV-Cry1-dVenus (*Right*) in the cultured SCN slice. (Scale bar: 100 μm.)

Movie S1

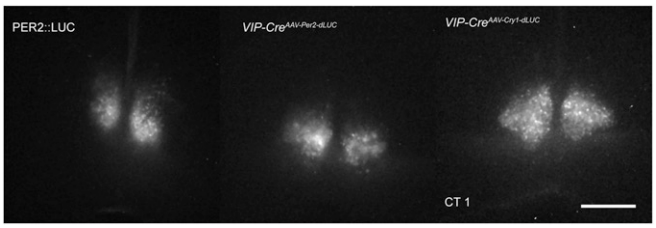

Movie S2. Representative images of circadian rhythms of PER2::LUC (*Left*), VIP-CreAAV-Per2-dLUC (*Middle*), and VIP-CreAAV-Cry1-dLUC (*Right*) in the cultured SCN slice. (Scale bar: 200 μm.)

Movie S2